Macromolecules

NOTE

pubs.acs.org/Macromolecules

Deformation-Induced Phase Separation in Blends of Poly(ε-caprolactone) with Poly(vinyl methyl ether)

Zhiyong Jiang,[†] Lianlian Fu,[†] Yingying Sun,[†] Xiuhong Li,[‡] and Yongfeng Men*[,†]

[†]State Key Laboratory of Polymer Physics and Chemistry, Changchun Institute of Applied Chemistry, Chinese Academy of Sciences, Renmin Street 5625, 130022 Changchun, P. R. China

[‡]SSRF, Shanghai Institute of Applied Physics, Chinese Academy of Sciences, 201800 Shanghai, P. R. China

Supporting Information

1. INTRODUCTION

Being composed of crystalline lamellae and the entangled amorphous polymeric chains in between, semicrystalline polymers always exhibit a complex behavior under tensile deformation.[1,2] The reaction of semicrystalline polymers upon deformation is generally affected by both the crystalline and the amorphous phase.[3−6] Moreover, the relative weights of the contributions from the two phases change with the extent of deformation.[7−15] As it turns out, the critical strain associated with the beginning of a disaggregation of the blocklike crystallites and recrystallization of the freed polymeric chain segments forming fibrils is related to the interplay between the amorphous entanglement density and the stability of crystal blocks.[3,4] Poly(ε-caprolactone) (PCL) is a semicrystalline polymer, which can form homogeneous mixtures in the melt and solution with a wealth of other noncrystallizable compounds, including poly(vinyl methyl ether) (PVME),[4,16] poly(styrene-*co*-acrylonitrile),[17,18] and poly(vinyl chloride).[19,20] PCL is, therefore, a natural candidate to investigate the effect of blending on the mechanical properties and deformation behavior, thus providing new insight into the role of the entangled amorphous network in the tensile deformation of semicrystalline polymers. A variety of reports were devoted to studying the variations of the kinetics of crystallization and spherulitic morphology of PCL in its blends with a noncrystallizable component.[21−23] Additionally, several groups addressed mechanical properties and deformation characteristics in PCL-based miscible blends under uniaxial tensile deformation utilizing true stress−strain measurements and infrared spectroscopy.[3,4,24,25] However, still limited attempts have been made to systematically evaluate the morphological evolution and deformation behavior of PCL-based miscible mixtures at the lamellar level under uniaxial extension.

In the present work, we study the microstructural evolution of PCL/PVME blends at the nanoscale as a function of blend composition and deformation ratio at room temperature using the in situ synchrotron small-angle X-ray scattering (SAXS) technique. As was found, the introduction of noncrystallizable PVME into the amorphous regions of PCL resulted in a shift of critical strain where the fibrillation just sets in to larger value because of the reduced network modulus of the amorphous phase. Moreover, a deformation-induced phase separation between PCL and PVME was observed after lamellar-to-fibrillar transition.

2. EXPERIMENTAL SECTION

Samples of PCL and PVME were supplied by Aldrich Chemical Co. The PCL had molecular weights of M_w = 65 000 g/mol and M_n = 42 500 g/mol. The PVME (M_w = 20 000 g/mol and a polydispersity index of 2.5) was obtained in the state of 50 wt % in water. PCL/PVME blends in different proportions were prepared in a THF solution. After sufficient evaporation of the solvent, samples for the measurements were prepared by compression molding at 100 °C followed by rapidly quenching the melt into ice water. In situ synchrotron SAXS measurements with a sample-to-detector distance of 1827 mm were performed at the beamline BL16B at SSRF, Shanghai, China. The synchrotron X-ray radiation had a wavelength of 0.124 nm. The samples were stretched stepwise at a constant crosshead speed of 0.6 mm/min, and SAXS patterns were collected within an accumulation time of 120 s after each step. Meanwhile, optical images of the deformed samples were recorded in order to measure the true strain at the position of X-ray beam. Wide-angle X-ray diffraction experiments were performed on a Rigaku X-ray diffractometer (D/max 2500) using imaging plate as X-ray detector.

Assuming a constant volume during elongation, the Hencky measure of the strain ε_H was used as a measure for the deformation. It is defined as

$$\varepsilon_H = 2 \ln \frac{b_0}{b} \tag{1}$$

where b_0 and b represent the widths of the undeformed and deformed areas located at specific spots on the samples.

Additionally, differential scanning calorimetry (DSC) measurements were conducted on samples before and after stretching. A DSC1 Star^e System (Mettler Toledo Instruments), which had been calibrated for temperature and melting enthalpy by using indium as a standard, was used during the experiments at a heating rate of 10 K/min.

3. RESULTS AND DISCUSSION

Figure 1 presents SAXS patterns of the pure PCL and its blends with PVME before and after uniaxial stretching. The characteristics of the evolution of the microstructure in the systems during stretching follow a common scheme as discussed before for typical semicrystalline polymers[26,27] and thus will not be discussed in detail in this short note. A detailed plot giving SAXS patterns as a function of strain is included in the Supporting Information (Figure S1). Besides the well-known phenomenon

Received: June 14, 2011
Revised: July 26, 2011
Published: August 15, 2011

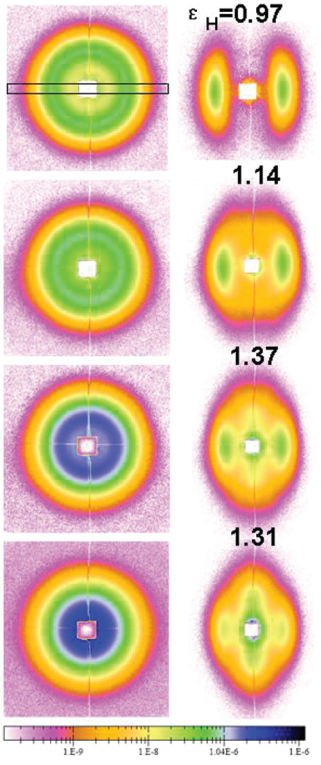

Figure 1. Selected small-angle X-ray scattering patterns of PCL/PVME blends measured before and after tensile deformation (from top to bottom: 100/0, 90/10, 80/20, and 70/30). The true strains for the deformed samples are indicated above each pattern. The stretching direction is horizontal and is defined as meridian direction.

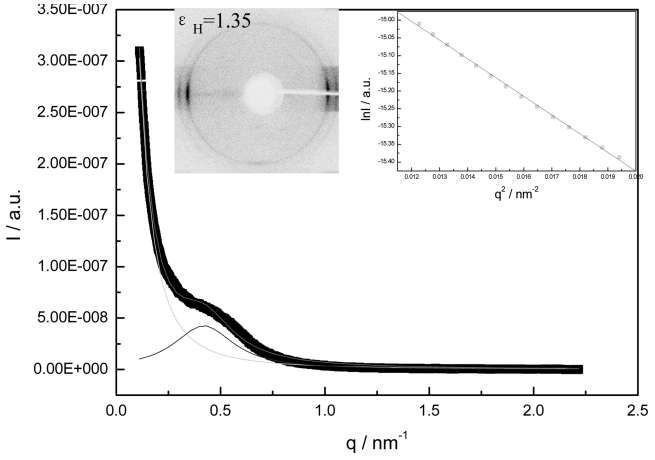

Figure 2. One-dimensional scattering intensity distribution of PCL/PVME blend with a content of 30 wt % PVME at a strain of 1.31 obtained by equatorial scan along the scattering streak across the beam stop and the decomposition into two contributions. The wide-angle X-ray diffraction pattern of the deformed PCL/PVME blend at a strain of 1.35 and the Guinier approximation are shown in the inset of the plot.

of changing from isotropic scattering patterns to strongly oriented ones after uniaxial deformation, Figure 1 shows another notable scattering character, namely the appearance of equatorial scattering streak passing through the beam center in blends with higher concentration of PVME. Such a scattering behavior indicates the formation of an elongated heterogeneous structure

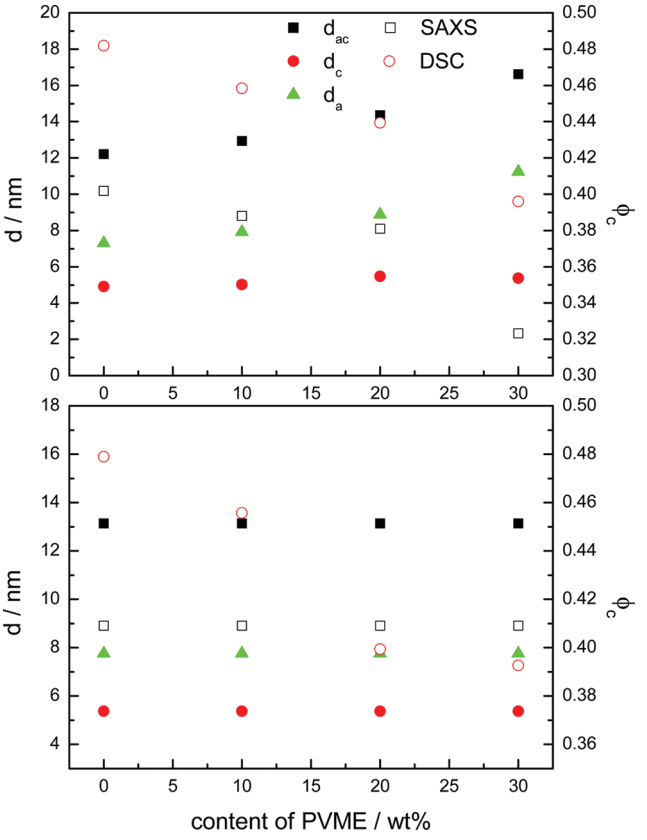

Figure 3. Evolution of the long spacing (d_{ac}) together with the average thicknesses of crystalline (d_c) and amorphous layers (d_a) as a function of PVME content measured for the series of PCL/PVME blends before (top) and after (bottom) uniaxial extension. The crystallinities calculated from both SAXS and DSC are also included in each plot.

of different electron density along the stretching direction such as fibrils or cavities. However, cavitation is ruled out in the present case because all samples show no strain whitening during stretching. If the scattering streak were due to cavities, the intensity would be much stronger than observed here. In addition, the yield stress decreases with increasing content of PVME (as shown in ref 4), and therefore the cavitation could be suppressed at higher volume fractions of PVME. Thus, this equatorial scattering streak can be assigned to the increased contrast between the fibrils and the interfibrillar materials. The wide-angle X-ray diffraction pattern (inset of Figure 2) clearly shows the existence of lamellar stacks with their normal perpendicular to the stretching direction after deformation. Because of survival of these crystalline lamellae after deformation, the scattering intensity distribution of the PCL/PVME blend obtained by equatorial scan along the scattering streak was decomposed into two contributions based on Lorentzian functions, as given in Figure 2. We tried to estimate the width of the fibrils using the Guinier approximation by considering the intensity distribution arising from the fibril scattering.[1,28] The calculation yields a value of about 12 nm. Note that the Guinier approximation is strictly applicable for monodisperse systems only when $qR < 1$ (R denotes the radius of gyration of the fibrils). This prerequisite is not fulfilled in our case where $q_{min} = 0.11$ nm^{-1}. The application of this formalism, however, gives at least a rough estimation of the fibrils dimension in their lateral direction. The scattering intensity distribution for stacks of lamellae was

dx.doi.org/10.1021/ma201346v |Macromolecules 2011, 44, 7062–7065

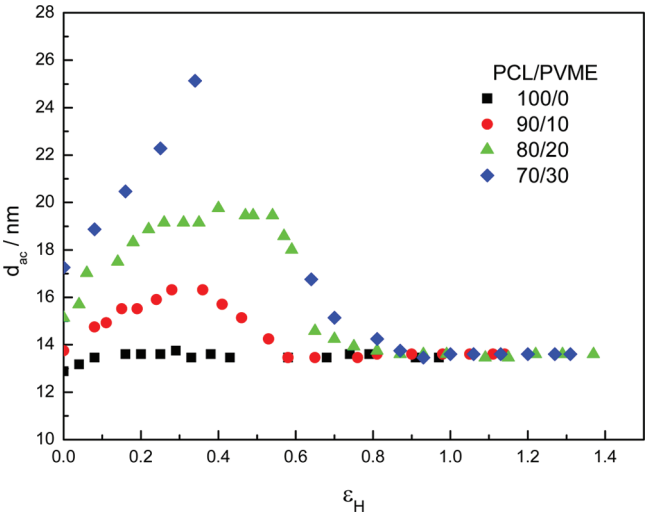

Figure 4. PCL/PVME blends: strain dependence of the long spacing d_{ac} along the drawing direction derived from Lorentz-corrected scattering curves.

Scheme 1. Schematic Representation of the Structural Evolution of the Pure PCL (Top) and Its Blends with PVME (Bottom) Subjected to Tensile Deformation at Room Temperature[a]

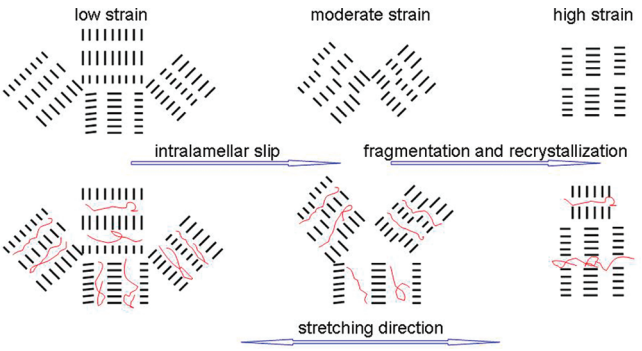

[a] The solid lines and red curves represent the PCL layer-like crystalline lamellae and PVME amorphous polymeric chains, respectively.

obtained by meridian scans along the stretching direction as schematically shown in the top left of Figure 1. The average thicknesses of the crystalline and amorphous layers as well as the long spacing measured along the stretching direction were derived from SAXS data using the one-dimensional correlation function. Figure 3 displays the evolution of these parameters together with the crystallinity as a function of PVME content before and after uniaxial stretching. As can be seen, the inclusion of a noncrystallizable component of PVME does not alter the thickness of crystalline lamellae (i.e., 5 nm) and leads only to a swelling of the amorphous phase of PCL prior to deformation. On the other hand, one observes an invariance of the long spacing together with the average thicknesses of the crystalline and amorphous layers with the blend composition in the necked zone after uniaxial stretching. In addition, the mass fraction of crystallites with respect to the total weight of blends was derived from the heat of fusion based on the melting enthalpy of hypothetical 100% crystalline PCL of 157 J/g (from ATHAS databank); the volume fraction of crystallites within the lamellar stacks (linear crystallinity) was evaluated from the ratio of the crystal thickness and the long spacing (d_c/d_{ac}). It must be mentioned that a comparison of the DSC crystallinity with the linear crystallinity can be employed to judge whether one deals with a homogeneous or a phase separated sample, due to density difference between the crystallites and the amorphous phase. As a result, it is clear that the noncrystallizable compound which had mixed with the amorphous phase of semicrystalline PCL was excluded from the oriented lamellar stacks under tensile deformation.

In order to represent the data of the isotropic samples with the correct weighting, the scattering intensity was multiplied by q^2 for data processing (Lorentz correction), whereas no Lorentz correction must be applied for the data with fiber symmetry, i.e., at high stretching ratios.[1,28,29] As pointed out in our previous studies, for a semiquantitative discussion of the dependence of the long spacing on the strain, the type of data treatment (Lorentz correction versus no correction) plays only a subordinate role.[26,27] Consequently, in the present work the values of the lamellar long spacings were derived from the Lorentz-corrected scattering curves along the stretching direction (Figure 4). When the content of PVME is raised to 30 wt %, the long spacing cannot be calculated between strain values of 0.4 and 0.6 due to a loss of the positional correlation between the crystalline lamellae with their normal along the drawing direction as seen in Figure S2. When the amorphous compound PVME is introduced, there is a considerable increase in the long spacing for all the mixtures in the initial stages of deformation, the extent of which depends on the content of PVME. Furthermore, it is evident that the critical strain, at which the crystalline blocks are no long stable and the formation of fibrils sets in, shifts to higher value with increasing concentration of PVME. This can be interpreted by assuming that the incorporation of PVME with different amount affects the state of the PCL amorphous phase to a different extent. The blend with a high content of PVME implies a reduced effective modulus of the entangled amorphous network because of a significant decrease of concentration of tie molecules and an increase in the concentration of chain ends that may easily be freed during deformation. Accordingly, the critical network stress, which is required to begin with a disintegration of the crystal blocks, is reached first for the mixture with a less amount of PVME.

Another important issue to be learned from Figure 4 is that the long spacing calculated after lamellar-to-fibrillar transition is essentially invariant, regardless of the concentration of PVME included in the blends. This behavior indicates that the amorphous PVME was introduced into the interfibrillar regions after fibrillation. Stretching of semicrystalline polymers is generally accompanied by a complete molecular rearrangement of the chain-folded lamellar morphology into a more or less chain-unfolded fibrillar microstructure at high draw ratios. Two distinct arguments have been proposed to account for the plastic nature underlying the lamellar-to-fibrillar transition, including crystal slips and stress-induced melting−recrystallization process.[30] On the basis of above observations, deformation-induced phase separation in the PCL/PVME blends can be viewed as an important evidence for the occurrence of stress-induced fragmentation and recrystallization at large strains. The structural evolution of PCL and its blends with PVME on the nanometer scale was elucidated in the process of deformation, as schematically represented in Scheme 1.

4. CONCLUSIONS

The microstructural evolution in the miscible blends of PCL with amorphous compound PVME was investigated as a function of true strain and blend composition using in situ synchrotron SAXS experiments. The critical strain marking the onset of lamellar-to-fibrillar transition shifted toward larger value with increasing content of PVME. This finding was ascribed to a reduced modulus of the entangled amorphous network after blending. With the progress of uniaxial extension, phase separation can be observed at high strains, which was induced by tensile deformation in the miscible blends of PCL with amorphous component PVME.

■ ASSOCIATED CONTENT

Supporting Information. Small-angle X-ray scattering patterns of samples deformed at different strain, one-dimensional integration of the scattering intensity along stretching direction, and DSC heating scans of samples before and after stretching. This material is available free of charge via the Internet at http://pubs.acs.org.

■ AUTHOR INFORMATION

Corresponding Author
*E-mail: men@ciac.jl.cn.

■ ACKNOWLEDGMENT

We acknowledge financial support from National Natural Science Foundation of China (50603024 and 50921062) and SSRF project 10sr0119.

■ REFERENCES

(1) Strobl, G. *The Physics of Polymers*, 2nd ed.; Springer: Berlin, Germany, 1997.
(2) Schultz, J. M. *Polymer Materials Science*; Academic Press: Englewood Cliffs, NJ, 1974.
(3) Men, Y. F.; Rieger, J.; Strobl, G. *Phys. Rev. Lett.* **2003**, *91*, 095502.
(4) Men, Y.; Strobl, G. *Macromolecules* **2003**, *36*, 1889.
(5) Jiang, Z. Y.; Tang, Y. J.; Rieger, J.; Enderle, H. F.; Lilge, D.; Roth, S. V.; Gehrke, R.; Heckmann, W.; Men, Y. F. *Macromolecules* **2010**, *43*, 4727.
(6) Bartczak, Z. *Macromolecules* **2005**, *38*, 7702.
(7) Hiss, R.; Hobeika, S.; Lynn, C.; Strobl, G. *Macromolecules* **1999**, *32*, 4390.
(8) Hobeika, S.; Men, Y.; Strobl, G. *Macromolecules* **2000**, *33*, 1827.
(9) Kennedy, M. A.; Peacock, A. J.; Failla, M. D.; Lucas, J. C.; Mandelkern, L. *Macromolecules* **1995**, *28*, 1407.
(10) Kennedy, M. A.; Peacock, A. J.; Mandelkern, L. *Macromolecules* **1994**, *27*, 5297.
(11) Butler, M. F.; Donald, A. M.; Bras, W.; Mant, G. R.; Derbyshire, G. E.; Ryan, A. J. *Macromolecules* **1995**, *28*, 6383.
(12) Butler, M. F.; Donald, A. M.; Ryan, A. *Polymer* **1997**, *38*, 5521.
(13) Liu, L. Z.; Hsiao, B. S.; Fu, B. X.; Ran, S. F.; Toki, S.; Chu, B.; Tsou, A. H.; Agarwal, P. K. *Macromolecules* **2003**, *36*, 1920.
(14) Toki, S.; Sics, I.; Burger, C.; Fang, D.; Liu, L.; Hsiao, B. S.; Datta, S.; Tsou, A. H. *Macromolecules* **2006**, *39*, 3588.
(15) Schrauwen, B.; Janssen, R.; Govaert, L.; Meijer, H. *Macromolecules* **2004**, *37*, 6069.
(16) Bisso, G..; Casarino, P.; Pedemonte, E. *Macromol. Chem. Phys.* **1999**, *200*, 376.
(17) Li, W.; Prud'homme, R. E. *Polymer* **1994**, *35*, 3260.
(18) Chiu, S. C.; Smith, T. G.. *J. Appl. Polym. Sci.* **1984**, *29*, 1797.
(19) Stein, R. S.; Khambatta, F. B.; Warner, F. P.; Russell, T.; Escala, A.; Balizer, E. *J. Polym. Sci., Polym. Symp.* **1978**, *63*, 313.
(20) Russell, T. P.; Stein, R. S. *J. Polym. Sci., Polym. Phys. Ed.* **1983**, *21*, 999.
(21) Wang, Z.; Jiang, B. *Macromolecules* **1997**, *30*, 6223.
(22) Wang, Z.; Wang, Y.; Yu, D.; Jiang, B. *Polymer* **1997**, *38*, 5897.
(23) Ong, C. J.; Price, F. P. *J. Polym. Sci., Polym. Symp.* **1978**, *63*, 45.
(24) Zhao, Y.; Keroack, D.; Prud'homme, R. E. *Macromolecules* **1999**, *32*, 1218.
(25) Keroack, D.; Zhao, Y.; Prud'homme, R. E. *Polymer* **1998**, *40*, 243.
(26) Jiang, Z. Y.; Tang, Y. J.; Men, Y. F.; Enderle, H. F.; Lilge, D.; Roth, S. V.; Gehrke, R.; Rieger, J. *Macromolecules* **2007**, *40*, 7263.
(27) Jiang, Z. Y.; Tang, Y. J.; Rieger, J.; Enderle, H. F.; Lilge, D.; Roth, S. V.; Gehrke, R.; Wu, Z.; Li, Z.; Men, Y. F. *Polymer* **2009**, *50*, 4101.
(28) Glatter, O.; Kratky, O. *Small-Angle X-ray Scattering*; Academic Press: London, UK, 1982.
(29) Crist, B.; Morosoff, N. *J. Polym. Sci., Polym. Phys.* **1973**, *11*, 1023.
(30) Séguéla, R. *e-Polym.* **2007**, *no. 032*.